REPORT DOCUMENTATION PAGE

AFRL-SR-AR-TR-08-0174

1. REPORT DATE *(DD-MM-YYYY)*	2. REPORT TYPE	...ES COVERED *(From - To)*
02/22/2007	FINAL	02/01/04 - 07/31/07

4. TITLE AND SUBTITLE

COMMUNICATION WITH HYPERSONIC VEHICLES VIA NONLINEAR PLASMA PROCESSES

5a. CONTRACT NUMBER

FA9550-04-1-0090

5b. GRANT NUMBER

N/A

5c. PROGRAM ELEMENT NUMBER

N/A

6. AUTHOR(S)

NEWELL, ALAN C, PhD
ZAKHAROV, VLADIMIR E, PhD

5d. PROJECT NUMBER

N/A

5e. TASK NUMBER

N/A

5f. WORK UNIT NUMBER

N/A

7. PERFORMING ORGANIZATION NAME(S) AND ADDRESS(ES)

Arizona Board of Regents
University of Arizona
888 N. Euclid Avenue, Room 510
Tucson, Arizona 85722-3308

8. PERFORMING ORGANIZATION REPORT NUMBER

FA9550-04-1-0090

9. SPONSORING/MONITORING AGENCY NAME(S) AND ADDRESS(ES)

AF Office of Scientific
875 North Randolph Road NA
AF Office of Scientific Suite 325, Room 3112
Research Arlington, VA 22203
Dr Arje Nachman/NE

10. SPONSOR/MONITOR'S ACRONYM(S)

N/A

11. SPONSOR/MONITOR'S REPORT NUMBER(S)

N/A

12. DISTRIBUTION/AVAILABILITY STATEMENT

UNCLASSIFIED AND UNLIMITED
Distribution A: Approved for public release

13. SUPPLEMENTARY NOTES

N/A

14. ABSTRACT

We wish to transmit messages to and from a hypersonic vehicle around which a plasma sheath has formed. For long distance transmission, the signal carrying these messages must be necessarily low frequency, typically 2 GHz, to which the plasma sheath is opaque. The idea is to use the plasma properties to make the plasma sheath appear transparent.

Numerical and analytical results show that it is possible to use proposed technique to receive GPS signal on the vehicle even using klystrons available on the open market. Transmission of the signal to the earth-based stations is also solved problem.

15. SUBJECT TERMS

communication, plasma, supersonic vehicle, nonlinear interaction, GPS reception

16. SECURITY CLASSIFICATION OF:			17. LIMITATION OF ABSTRACT	18. NUMBER OF PAGES	19a. NAME OF RESPONSIBLE PERSON
a. REPORT	b. ABSTRACT	c. THIS PAGE			ALAN NEWELL
U	U	U	UU	26	19b. TELEPHONE NUMBER *(Include area code)* (520)626-4885

Final report on

"Communication with Hypersonic Vehicles Via Nonlinear Plasma Processes"

Grant AFOSR FA9550-04-1-0090

I. DESCRIPTION OF THE PROJECT.

A. Desired result.

The final goal is to devise means to maintain continuous contact with the hypersonic vehicle. When such vehicles were principally spacecrafts, a blackout period of up to two minutes was acceptable albeit undesirable. But when the vehicles are of military origin, it is clear that continuous contact is essential for both targeting and rapid abort reasons.

B. Challenge.

A vehicle moving through the stratosphere (altitudes 40km-50km) at hypersonic velocities (8-15 Mach) is covered by a plasma sheath. Typically, the plasma density n can be as high as $10^{18}m^{-3}$ with corresponding plasma frequency

$$2\pi f_L = \omega_L = \left(\frac{e^2 n}{M\varepsilon_0}\right)^{1/2} \tag{1}$$

of about $9GHz$. In (1), e is the electron charge $-1.6 \times 10^{-19}C$, $\varepsilon_0 = 8.85 \times 10^{-12}CV^{-1}m^{-1}$ and M is the electron mass $9 \times 10^{-31}kg$. Therefore the plasma is opaque to frequencies lower than $9GHz$. Direct communication through such a plasma to and from the vehicle is impossible because frequencies f suitable for long distance propagation through the atmosphere are usually much less. For example, the standard frequency used for navigational satellite systems, including the global positioning system (GPS), are less than $2GHz$. For the GPS, $f = 1.57542GHz$.

C. Review of solutions.

It is a challenge which has drawn many responses. They fall into several categories. The first ignores the presence of the plasma by using signals with frequencies well above the plasma frequency. The difficulty with this method is that such signals are heavily attenuated in and scattered by the atmosphere. A second means, which also ignores the plasma, is to use low frequency signals in the $100MHz$ range where wavelengths are large compared to the plasma sheath thickness (typically of the order of a meter). But such solutions have high cost and low bit rates and are not well supported by existing infrastructure. A third

category of solutions violates the plasma. One approach is to remove, by vehicle reshaping, for example, the plasma from certain points on the vehicle at which one might place an antenna. Another is to destroy it by electrophilic injection or by injecting water drops. A third approach is to use powerful magnets to reshape the plasma. Such solutions involve a heavy cost in that design features necessary for their implementation must be built into the vehicle a priori. Nevertheless some are feasible and worthy of consideration. For example, it is possible to build an antenna into a sharp leading edge which would protrude beyond the plasma and survive for sufficiently long (it would be eventually destroyed by ablation) to cover the flight time.

D. The most attractive and perspective solution.

The fourth category of solutions, and the one to which we are attracted, uses the properties of the plasma itself to effect transmission in the same way a judo expert uses the strength and motion of an opponent to defeat him. One idea is to create new modes of oscillation and propagation by the introduction of magnetic fields. Indeed, for strong enough fields, the Larmor frequency f_{Larmor} is sufficiently large that the window $(f_{Larmor}, \max(f_L))$ for which the plasma is opaque is small and transmission can be achieved for frequencies below f_{Larmor}. But the introduction of magnetic fields involves large additional weight and new design features. The second idea is much more simple. Its aim is to take advantages of nonlinear properties of plasma to render it effectively transparent to the signal. Communications both to and from the vehicle are feasible using basically the same ideas. We shall first describe the "to the vehicle" case. Consider Figure 1 in which we show schematically the response of the plasma to an incoming signal with low frequency ω from a direction which makes an angle ϕ with the normal to the vehicle. There are two principal features to the response. First, there is a reflection from the layer at a point $z = z_r$ where the plasma frequency at the point $\omega_L(z_r)$ is $\omega \cos\phi$. However, the influence of the signal is felt beyond that point, namely at the resonant layer $z = 0$ where $\omega_L(0) = \omega$. Langmuir oscillations are excited there which produce large transversal and longitudinal components of the electric field. The resonant layer acts as an antenna. The task is to find a way to connect the antenna at the resonant layer at $z = 0$ to a receiver on board the vehicle at $z = R$. There are several possibilities which we have outlined before [1–3].

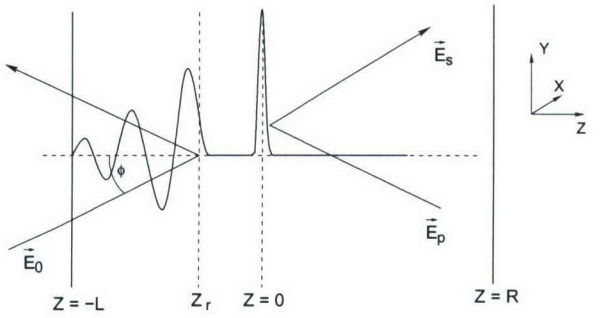

FIG. 1: $\omega_L(z_r) = \omega\cos\phi, \omega_L(0) = \omega$. If the thickness of the plasma sheath is equal to $L + R = 1m$, the signal frequency $f = 2GHz$ and the plasma frequency $f_L \simeq 9GHz$ then $L \simeq 5cm$ and $R \simeq 95cm$.

The most practical one, however, is also the most simple and first suggested without a detailed numerical simulation in [1]. We use an onboard source, which we call the pump, to generate electromagnetic signals of sufficiently high frequency ω_p ($\omega_p > \max_z \omega_L(z) + \omega$) that they can propagate through the plasma. There are several candidates for such a source. For example, available on the open market is a klystron amplifier which can generate $3kW$ of power at frequencies of $12 - 14GHz$. These high frequency waves have only to travel distances of a meter or less. They interact nonlinearly with and scatter off the signal wave. Not surprisingly, the largest contribution to the scattered wave comes from the nonlinear interaction of the pump wave with the plasma density distortion induced by the incoming signal wave at the resonant layer. We call the scattered wave a Stokes wave because the scattering process is a three wave interaction analogous to Raman scattering. The Stokes wave with frequency $\omega_S = \omega_p - \omega$ carries the information encoded on the signal wave back to the vehicle. We will show that, whereas much of the scattered Stokes wave propagates away from the vehicle, a significant fraction is returned to the vehicle.

What is remarkable is this. The ratio of the power flux of the Stokes wave received at the vehicle to the power flux contained in the signal wave at the plasma edge can be between 0.7 and 2 percent. This means that reception of GPS signals may be possible because one simply needs an onboard receiver approximately 100 times more sensitive than commercially available hand held receivers or use sufficiently larger antenna. We shall discuss in the Results section the sensitivity required for a variety of sources.

Communications from the vehicle requires two power sources on the vehicle. One, which

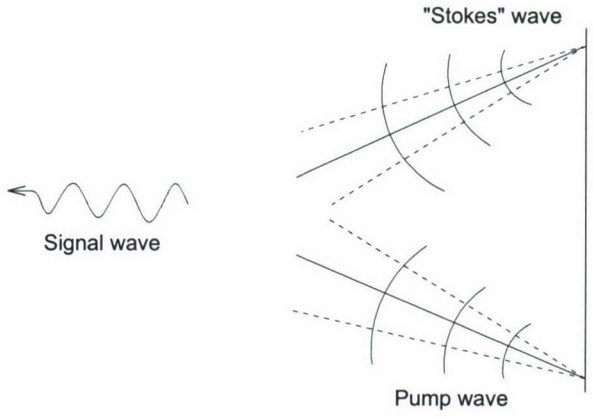

FIG. 2: The concept for communication from the vehicle. Although drawn in such a way that the angles of pumping, Stokes and signal waves are different, the optimal configuration is when all angles are the same, i.e. Stokes and pump waves are generated in the same direction as the target of the desired low frequency signal.

we term the Stokes wave generator, will also carry the signal. The other is the pump wave. Both have carrier frequencies above that of the maximum of the plasma frequency. Their nonlinear interaction in the plasma produces an oscillations of frequency $\omega = \omega_p - \omega_S$. Consider Figure 2. For $z_r < z < R$ where z_r is determined by $\omega_L(z_r) = \omega \cos\phi$ and ϕ is calculated from the differences in propagation directions of the pump and Stokes waves, the oscillation does not propagate and its strength decays away from the vehicle. Nevertheless this oscillation is sufficiently strong to act as a power source for a propagating wave in the region $z < z_r$ where $\omega \cos\phi > \omega_L(z)$. In the conclusion we analyze what power is required in order for the signal to be detected by distant receivers. It appears that even if we use usual available on the market generators communication can be put into practice.

II. OUR RESULTS.

A. Equations considered.

We begin with a detailed analysis of the two dimensional propagation and interaction of a signal wave of frequency ω, a pump wave of frequency ω_p and a Stokes wave of frequency ω_S through a plasma with a given density profile $n_0(z)$ where z is the direction normal to

the vehicle. The key equation is a modification of the well known Ginzburg equation [4]

$$\frac{\partial}{\partial z}\left(\left(\frac{\varepsilon_0}{\varepsilon(z,\Omega)}\right)\frac{\partial \vec{H}}{\partial z}\right)+\frac{\varepsilon_0}{\varepsilon(z,\Omega)}\frac{\partial^2 \vec{H}}{\partial y^2}+\frac{\Omega^2}{c^2}\vec{H}= \tag{2}$$
$$=-\left[\nabla\times\left(\frac{\varepsilon_0}{\varepsilon(z,\Omega)}\vec{j}_{NL}\right)\right],$$

for the magnetic field amplitude $(H(y,z),0,0)\mathrm{e}^{-\mathrm{i}\Omega t}$ of an oscillation of frequency Ω. In (2), the effective electric susceptibility is

$$\varepsilon(z,\Omega)=\varepsilon_0\left(1-\frac{\omega_L^2(z)}{\Omega^2}\left(\frac{1}{1+\mathrm{i}\nu/\Omega}\right)\right), \tag{3}$$

($\omega_L(z)$ is the local plasma frequency and ν the collision frequency). The susceptibility is due to the linear response of the plasma to the electric fields of whichever waves are involved. The nonlinear current $\vec{j}_{NL}$ will be determined both by the product of the plasma density distortion with the linear current and the nonlinear response of the electric velocity field due principally to dynamic pressure forces. We observe that, for $\Omega \gg \max_z \omega_L(z)$, the electric susceptibility is approximately ε_0 and the left hand side of the nonlinear Ginzburg equation (2) is the usual wave operator.

How do we use (2)? For the case of communication to the vehicle, we use it in two ways. First with $\vec{j}_{NL}=0$, we determine for $\Omega=\omega$ and $H(y,z)=H(z)\mathrm{e}^{\mathrm{i}(\omega/c)y\sin\phi}$, the field $H(z)$ from which the distortion to the plasma produced by the incoming wave is calculated. In this instance, $H(z)$ satisfies

$$\frac{d^2H}{dz^2}-\frac{1}{\varepsilon(z,\omega)}\frac{d\varepsilon(z,\omega)}{dz}\frac{dH}{dz}+ \tag{4}$$
$$\frac{\omega^2}{c^2}\left(\frac{\varepsilon(z,\omega)}{\varepsilon_0}-\sin^2\phi\right)H=0.$$

A glance at the third term shows that propagation is impossible for $\varepsilon/\varepsilon_0<\sin^2\phi$ or, from (3), for $\omega\cos\phi<\omega_L(z)$. The importance of the resonance layer where $\varepsilon(z,\omega)\simeq 0$ is seen from the denominator in the second term. Having solved for $H(z)$ from (4) we can then calculate the plasma distortion field $\delta n(z)$. Its interaction with the pumping wave then produces a nonlinear current $\vec{j}_{NL}$ which gives rise to the Stokes wave. The Stokes wave $H_S(y,z)$ and its propagation is calculated by solving (2) with this $\vec{j}_{NL}$ and appropriate boundary conditions at the plasma edge and at the vehicle. Our goal is to determine $H_S(y,z=R)$. We give the results of both the numerical simulation and an analytic estimation. The latter takes

advantage of the fact, that, for the Stokes wave, $\omega_S \gg \max_z \omega_L(z)$ and that the principal plasma distortion occurs at the resonance layer.

For communicating from the vehicle, we solve (4) with the right hand side given by $-\nabla \times \frac{\varepsilon_0}{\varepsilon}\vec{j}_{NL}$ with $\vec{j}_{NL}$ calculated from the nonlinear interaction of the pump and Stokes waves. Here the goal is to calculate the flux of power of the signal wave with frequency $\omega = \omega_p - \omega_S$ as it leaves the plasma edge in the direction of some distant receiver.

B. Analytic estimations.

1. *Model.*

We shall study a very idealized situation when the plasma sheath is a flat slab. The plasma density is a linear function of the horizontal coordinate z

$$n_0(z) = n_0 \frac{z+L}{R+L}. \tag{5}$$

In this geometry the vehicle is the vertical wall placed at $z = R$. The plasma density near the vehicle is n_0. The plasma contacts the vacuum at $z = -L$, where $n = 0$. We shall study two situations: communication to the vehicle and communication from the vehicle. In both cases, three almost monochromatic electromagnetic waves exist in the plasma. Two of them have high frequencies ω_p (pumping wave), ω_S (Stokes wave). The third one has low frequency ω, satisfying the condition

$$\omega = \omega_p - \omega_S. \tag{6}$$

In the "to the vehicle" case ω is the circular frequency of the incoming signal. In the "from the vehicle" case, ω is the circular frequency of the outgoing signal. In both these cases, the low-frequency signal plays a key role. Because the local plasma frequency at $z = 0$ is ω,

$$\omega^2 = \frac{e^2 n_0}{M\varepsilon_0} \frac{L}{R+L}. \tag{7}$$

Let us denote also the Langmuir frequency at the vehicle as

$$\omega_L^2 = \frac{e^2 n_0}{M\varepsilon_0}.$$

Thus

$$\frac{L}{R+L} = \frac{\omega^2}{\omega_L^2} = \frac{f^2}{f_L^2}.$$

In a realistic situation $f_L \simeq 9GHz$ (it corresponds to $n_0 = 10^{18}m^{-3}$), $f \simeq 2GHz$, $R + L = 1m$, and $L \simeq 0.05m$. The wavelength of the incoming signal in the vacuum is $\lambda = c/f = 0.15m$, so that $\lambda > L$. We point out that in the case of low-frequency wave reflection from the ionosphere, the situation is the opposite $\lambda << L$.

We shall assume that the ions' positions are fixed and the plasma is cold ($T_e \simeq 0$). The magnetic field has only one component H_x. The electric field has two components E_y, E_z. Neither the electric nor magnetic fields depend on the x-coordinate.

2. "To the vehicle."

We would like to estimate the ratio

$$\mu_S = \frac{S_S(z = R)}{S_0}$$

of the fluxes of the squared scattered field to the squared incoming signal field and express it as a function of pump power flux S_p measured in Watts per square meter.

We can make an analytic estimation of the three-wave process efficiency. The main contribution comes from the vicinity of $z = 0$. The reason comes from the fact that the real part of dielectric susceptibility (3) for the low frequency signal wave has a zero at this point. It means that our nonlinear current on the right hand side of the Ginzburg equation has a very sharp peak near $z = 0$. A typical plot of right hand side is given in Figure 3. This

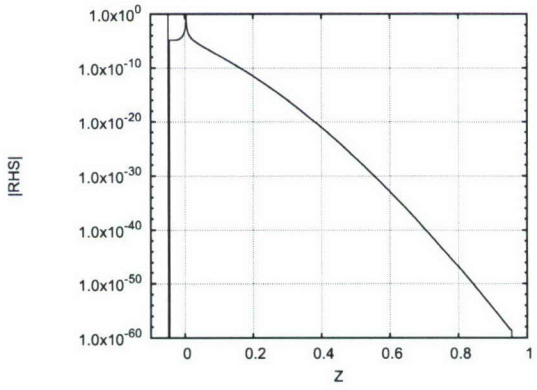

FIG. 3: The typical right hand side (absolute value) of the Ginzburg equation in the "to the vehicle" case. Logarithmic scale. One can see that the main contribution comes from the region of the point $z = 0$.

issue is discussed in more detail in Appendix A 2.

If we consider a high frequency pumping wave we can use the plane wave approximation

$$H_p(y,z,t) = H_p e^{\mathrm{i}(-\omega_p t + k_p y - \kappa_p z)}.$$

The low frequency signal wave can be written

$$H_0(y,t) = H(y,z,t)|_{z=0} = H(z)|_{z=0} e^{\mathrm{i}(-\omega t + k y)}.$$

For the Stokes wave, whose frequency is higher than the plasma frequency, one can use the following approximate Ginzburg equation

$$\frac{\partial^2 H_S}{\partial z^2} + \kappa^2 H_S = f_S, \tag{8}$$

where f_S is calculated from the curl of the nonlinear current. To solve, we use the method of variation of constants.We find

$$\begin{aligned} H_S &= C_1 e^{\mathrm{i}\kappa_S z} + C_2 e^{-\mathrm{i}\kappa_S z}, \\ C_1' e^{\mathrm{i}\kappa_S z} + C_2' e^{-\mathrm{i}\kappa_S z} &= 0, \\ C_1(z) &= \frac{1}{2\mathrm{i}\kappa_S} \int_{-L}^{z} e^{-\mathrm{i}\kappa_S y} f_S(y) dy, \\ C_2(z) &= -\frac{1}{2\mathrm{i}\kappa_S} \int_{z}^{R} e^{\mathrm{i}\kappa_S y} f_S(y) dy. \end{aligned}$$

One can say that C_1 is the amplitude of the Stokes wave propagating to the vehicle and C_2 is the amplitude of the anti-Stokes wave propagating from the vehicle. The main contribution to $C_1(R)$ arises from the vicinity of $z = 0$, where $f_S(z)$ is almost singular

$$\begin{aligned} C_1(R) &= \frac{1}{2\mathrm{i}\kappa_S} \int_{-L}^{R} f_S(y) e^{-\mathrm{i}\kappa_S y} dy \simeq \\ &\simeq \frac{1}{2\mathrm{i}\kappa_S} \int_{-\infty}^{+\infty} f_S(y) e^{-\mathrm{i}\kappa_S y} dy. \end{aligned}$$

After some simple but tedious calculations (see Appendix A 2) one finds

$$C_1(R) \simeq 2\pi \mathrm{i} \frac{eL}{Mc^2} \frac{1}{\varepsilon_0 c} \cos(2\theta) \sin(\phi) H_p H^*(0). \tag{9}$$

where θ is the pumping incident angle.

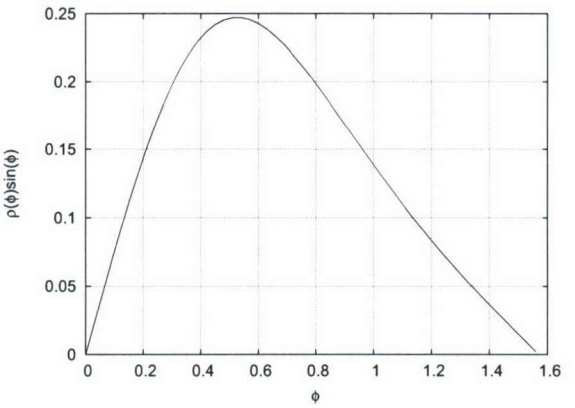

FIG. 4: Dependence of $C_1(R)$ on the signal incidence angle ϕ.

Details of these calculations are given in Appendix A 2. The angular dependence of $H(0)$, which we call $\rho(\phi)$, can be calculated numerically by solving the homogeneous Ginzburg equation. In Fig. 4, we plot the product $\rho \sin\phi$ against ϕ. At the optimal value $\phi \simeq 0.5$, $\rho(\phi)\sin\phi \simeq 1/4$,

$$C_1(R) \simeq \frac{\pi}{2} \mathrm{i} \frac{eL}{Mc^2} \frac{1}{\varepsilon_0 c} \cos 2\theta H_p H^*(-L). \tag{10}$$

Using the expression $S_p = |H_p|^2/(\varepsilon_0 c)$, one gets

$$\mu_S = \left|\frac{C_1}{H}\right|^2 c\varepsilon_0 \frac{S_p}{1Wm^{-2}} \simeq$$
$$\simeq \frac{\pi^2}{4} \left(\frac{eL}{Mc^2}\right)^2 \frac{1}{\varepsilon_0 c} \cos^2(2\theta) \frac{S_p}{1Wm^{-2}}. \tag{11}$$

For the optimal values of incidence angles ($\theta = 0$, $\phi \simeq 0.5$), the given plasma parameters and $L \simeq 0.05m$, one gets the following maximum value of the efficiency coefficient

$$\mu_S \simeq 0.9 \times 10^{-11} \frac{S_p}{1Wm^{-2}}. \tag{12}$$

This is consistent with what we obtain by direct numerical simulation.

3. "From the vehicle."

Equation (2) can be rewritten in the following form

$$\frac{\mathrm{d}}{\mathrm{d}z} \frac{1}{\varepsilon} \frac{\mathrm{d}H}{\mathrm{d}z} + \left(\frac{1}{\varepsilon_0} \frac{\omega^2}{c^2} - \frac{k_0^2}{\varepsilon_0}\right) H = \frac{\partial}{\partial z} \left(\frac{(\vec{j}_{NL})_y}{\varepsilon}\right) - \tag{13}$$
$$- \frac{1}{\varepsilon} \frac{\partial}{\partial y} (\vec{j}_{NL})_z.$$

It is not too surprising that that the dominant contribution to the RHS of (13) is the first term and arises from the neighborhood of $z = 0$. Again, just as in the "to the vehicle" case, the resonant layer acts as a transmitting antenna which will beam the message contained on the Stokes wave to a distant receiver at frequency $\omega = \omega_p - \omega_S$. the dominant contribution comes from the first term on the RHS of (13) and from the neighborhood of $z = 0$.

If we consider the expression for $(\vec{j}_{NL})_y$ given in Appendix A, we can see that in the case $\omega_0 \ll \omega_S, \omega_p$ the first term (A5) is the major one in the vicinity of resonant layer. The resonant layer works like radiating antenna.

Using the simplified nonlinear current expression and considering the pumping and Stokes waves as plane waves one finds

$$H(-L) \simeq -\mathrm{i}\frac{e\omega_0^2 L \sin\phi}{2M\varepsilon_0 c^3 \omega_S \omega_p}\frac{1}{A} H_p H_S^* \times \tag{14}$$
$$\times \frac{\phi_1'(-L)}{\phi_1'(-L) + \mathrm{i}\kappa_0\phi_1(-L)}\left(1 - \frac{\mathrm{e}^{\mathrm{i}A\cos\phi} - 1}{A\cos\phi}\right).$$

Where $A = L\omega_0/c$.

Using the solutions of the approximate homogeneous equations, we can estimate $\phi_1'(z)/\phi_1(z)|_{z=-L} \simeq 1/L$. Thus for $\kappa_0 L = A\cos\phi \ll 1$, one finds

$$H(-L) \simeq \frac{e\omega_0^2 L \sin\phi}{4M\varepsilon_0 c^3 \omega_S \omega_p}\frac{1}{A} H_p H_S^*.$$

For the power density, we have

$$S = \frac{1}{32}\left(\frac{eL}{Mc^2}\right)^2 \frac{1}{\varepsilon_0 c}\left(\frac{\omega_0^2}{\omega_S\omega_p}\right)^2 \sin^2\phi S_S S_p. \tag{15}$$

This result is quite clear from physical point of view. The larger ϕ is, the longer is the distance over which the signal wave is generated in the plasma.

In our simulations, $A \simeq 2.1$ and in this case we cannot use the simplified expression given above. Instead we find,

$$S = \frac{1}{8}\left(\frac{eL}{Mc^2}\right)^2 \frac{1}{\varepsilon_0 c}\left(\frac{\omega_0^2}{\omega_S\omega_p}\frac{1}{A}\right)^2 \times$$
$$\times \tan^2\phi\left(1 - 2\frac{\sin(A\cos\phi)}{A\cos\phi} + 2\frac{1-\cos(A\cos\phi)}{A^2\cos^2\phi}\right) \times \tag{16}$$
$$\times \frac{1}{1 + C_{der}\cos^2\phi} S_S S_p.$$

Here we introduced the coefficient $C_{der} = (\kappa_0\phi_1/\phi_1')^2$ the value of which we obtain from our numerics.

Finally, we find

$$S_{12GHz} = 1.2 \times 10^{-16} \tan^2\phi \left(1 - 2\frac{\sin(A\cos\phi)}{A\cos\phi} + \right.$$
$$\left. + 2\frac{1-\cos(A\cos\phi)}{A^2\cos^2\phi}\right) \frac{1}{1 + C_{der}\cos^2\phi} S_S S_p, \tag{17}$$

$$S_{18GHz} = 2.0 \times 10^{-17} \tan^2\phi \left(1 - 2\frac{\sin(A\cos\phi)}{A\cos\phi} + \right.$$
$$\left. + 2\frac{1-\cos(A\cos\phi)}{A^2\cos^2\phi}\right) \frac{1}{1 + C_{der}\cos^2\phi} S_S S_p. \tag{18}$$

The subscripts refer to the frequencies of the onboard pump waves. Again, we find the magnitude and angular dependence to be consistent with our numerical results.

C. Numerical simulations.

The equation we solve numerically in all cases is the Ginzburg equation (2) including all terms on its right hand side. The boundary conditions are given at $z = L_1 = -L - (L + R)$, in the vacuum beyond the plasma edge and at $z = R$, the vehicle.

We tested the robustness of the code by allowing for both finite and zero conductivity of the vehicle surface in the "to the vehicle case". During the simulation in the "from the vehicle" case we also redid the simulation with the derivative of the magnetic field at the vehicle equal to zero. In all the cases, the influences of the differing boundary conditions were negligible.

1. "To the vehicle."

As the first step in the "to the vehicle" case we have to find the profile of the incoming magnetic field in the plasma. We used an incident angle $\phi = 0.5$. It will be shown later that this angle is an optimal value but it is good for an initial evaluation of the possibility of communication. We consider the incoming signal as a monochromatic plane wave of a given frequency $f_0 = 2GHz$ and amplitude H_0. The current is equal to zero. In this case, the boundary conditions are

$$z = -L_1, \quad \frac{\partial H}{\partial z} + \mathrm{i}\kappa_0 H = 2\mathrm{i}\kappa_0 H_0, \tag{19}$$

$$z = R, \quad \frac{\partial H}{\partial z} = 0. \tag{20}$$

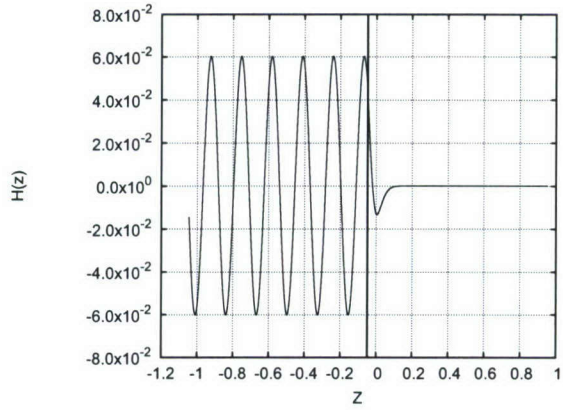

FIG. 5: Incoming signal magnetic field profile.

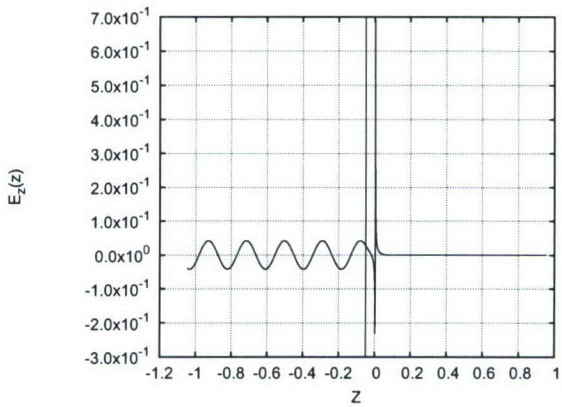

FIG. 6: Incoming signal electric field (z-component) profile.

The resulting profile of the magnetic field is shown in Fig. 5. The profile of $E_z(z)$ is shown in Fig. 6. At the next stage, we consider an incident low frequency magnetic field profile as a source of distortion of the plasma density profile and take into account currents due to the presence of a pump wave. The pumping wave angle $\theta = 0.0$. Our goal is to calculate the scattered field H_S with frequency $\omega_S = \omega_p - \omega$. In this case, the boundary conditions are

$$z = -L_1, \ \frac{\partial H_S}{\partial z} + \mathrm{i}\kappa_S H = 0, \tag{21}$$

$$z = R, \ \frac{\partial H_S}{\partial z} = 0. \tag{22}$$

The profiles of the magnetic fields H_S for two different pumping frequencies are shown in Figures 7 and 8. We note that the resonant layer $z = 0$ acts as if it were a source. In the

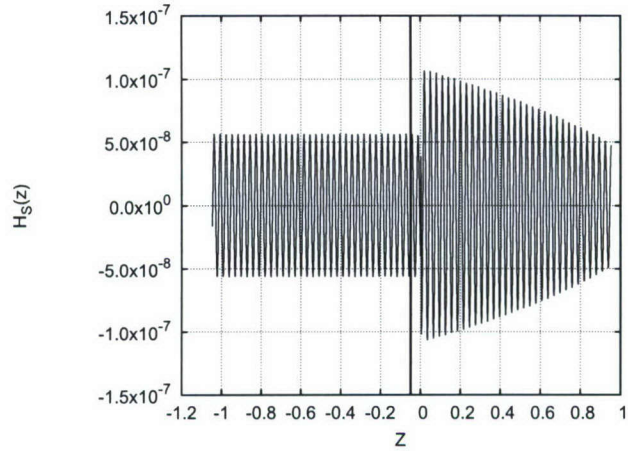

FIG. 7: Magnetic field profile of the Stokes wave. Pumping frequency 12GHz.

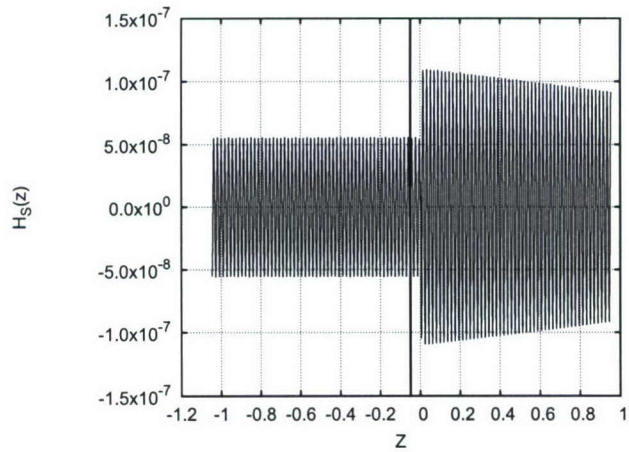

FIG. 8: Magnetic field profile of the Stokes wave. Pumping frequency 18GHz.

"to the vehicle" case, it is convenient to introduce the function μ_S as the ratio

$$\mu_S = \frac{S_S(z=R)}{S_0}$$

of the scattered field flux to the incoming signal flux and express it as a function of pump flux S_p measured in Watts per square meter. We found

$$\omega_p = 2\pi * 12GHz,\ \max(\mu_S) \simeq 2.2 \times 10^{-12} \frac{S_p}{1Wm^{-2}},$$

$$\omega_p = 2\pi * 18GHz,\ \max(\mu_S) \simeq 0.63 \times 10^{-11} \frac{S_p}{1Wm^{-2}}.$$

These results are in a good agreement with the analytic estimation (12). Any difference is due to the fact that the pumping frequency is not sufficiently high to neglect the plasma

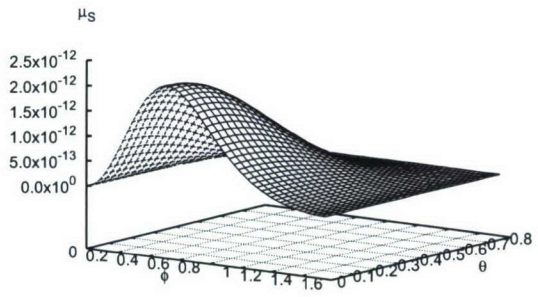

FIG. 9: Dependence of power conversion efficiency coefficient μ_S on angles. "To the vehicle". Pumping frequency 12GHz.

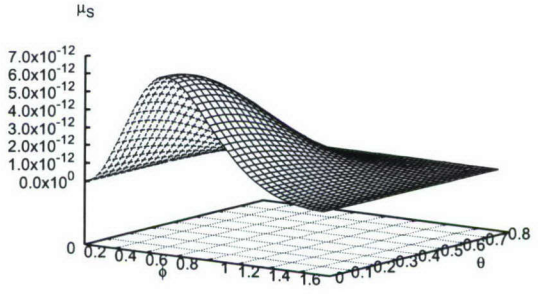

FIG. 10: Dependence of power conversion efficiency coefficient μ_S on angles. "To the vehicle". Pumping frequency 18GHz.

frequency. The reason we used these frequencies and not much higher ones was that they are available on standard microwave equipment and devices.

In order to investigate the dependence of the result on the angles ϕ, θ_p, θ_S, we calculated μ for various different choices. The results are shown in Figs. 9-10.

As one can see, in the "to the vehicle" case we have a very good agreement between the analytically estimated angular dependence (11) and the numerical results. Namely, we have a maximum at pumping angles close to $\theta = 0$ and the efficiency coefficient μ_S goes to zero at the vicinity of $\theta = \pi/4$ in a agreement with the $\cos(2\theta)$ dependence. So we can formulate a simple rule: in order to get the best possible performance, send the pump wave in a direction perpendicular to the plasma edge surface.

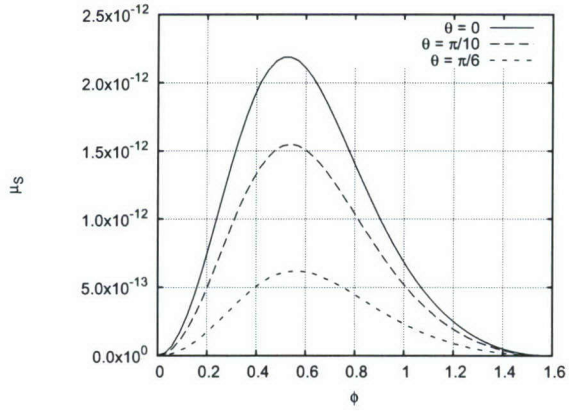

FIG. 11: Dependence of the power conversion efficiency coefficient μ_S on several pumping angles, in the "to the vehicle" case. Pumping frequency 12GHz.

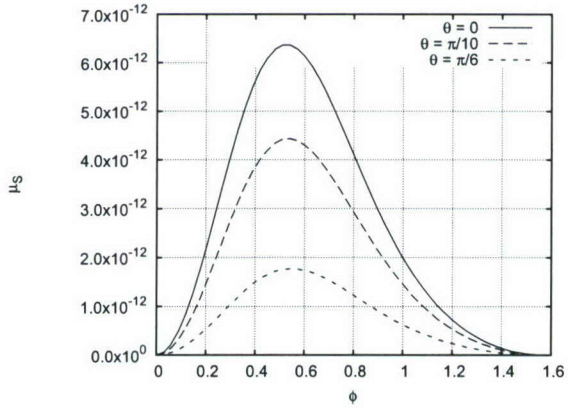

FIG. 12: Dependence the of power conversion efficiency coefficient μ_S on several pumping angles, in the "to the vehicle" case. Pumping frequency 18GHz.

2. "From the vehicle."

In the "from the vehicle" case we calculate the magnetic field of the low frequency wave generated by plane pump and Stokes waves. Following the optimal strategy in this case, described in the analytic part of the paper, we take all angles equal to each other $\phi = \theta = \pi/4$. In this case, the boundary conditions are

$$z = -L_1, \ \frac{\partial H}{\partial z} + \mathrm{i}\kappa_0 H = 0, \tag{23}$$

$$z = R, \ H = 0. \tag{24}$$

Here $H(z)$ is the magnetic field of the signal wave with frequency $\omega = \omega_p - \omega_S$. The boundary condition at $z = R, \ H = 0$, gives us the worst of all cases by definition.

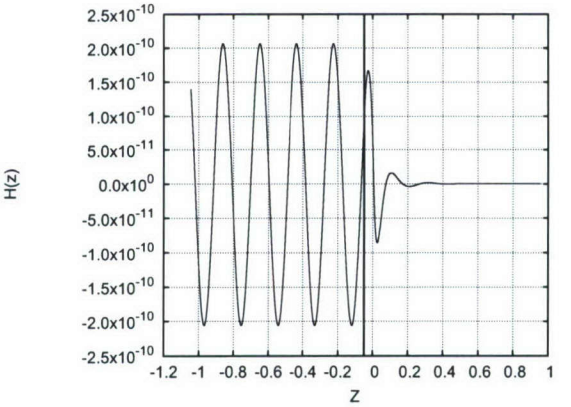

FIG. 13: Generated low frequency magnetic field. Pumping frequency 12GHz.

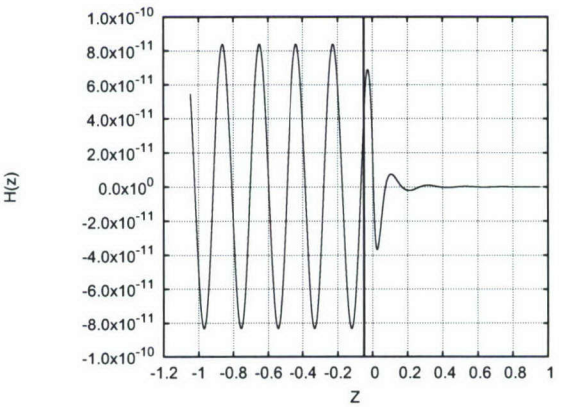

FIG. 14: Generated low frequency magnetic field. Pumping frequency 18GHz.

The low frequency magnetic fields for two different pumping frequencies are shown in Figs. 13 and 14. In the "from the vehicle" case, we calculate the ratio

$$\mu = \frac{S_{out}(z=-L)}{S_S S_p}$$

of the output signal flux to the product of the pump and Stokes fluxes and express it as a function of the optimal angle.

We found

$$\omega_P = 2\pi * 12GHz,\ \max(\mu) \simeq 1.8 \times 10^{-16} \frac{1}{1Wm^{-2}},$$

$$\omega_P = 2\pi * 18GHz,\ \max(\mu) \simeq 3.0 \times 10^{-17} \frac{1}{1Wm^{-2}}.$$

In order to investigate the dependence of the result on the angles ϕ, θ_p, θ_S, we calculated μ for various different choices. The results are shown in Figs. 15-16.

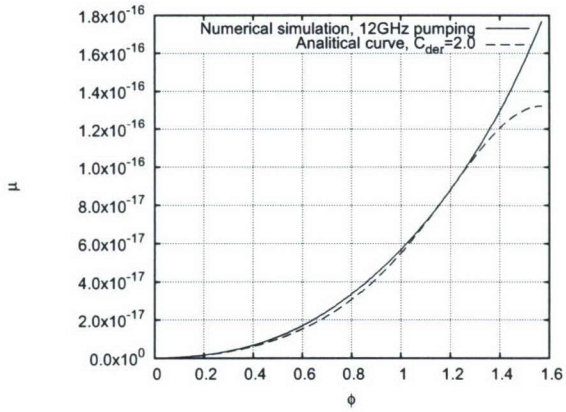

FIG. 15: Dependence of the power conversion efficiency coefficient μ on optimal angle. "From the vehicle". Pumping frequency 12GHz.

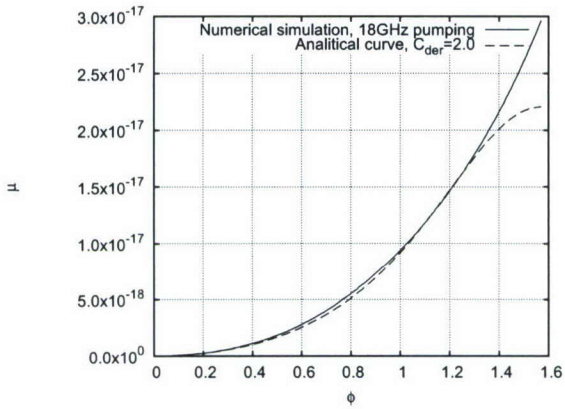

FIG. 16: Dependence of power conversion efficiency coefficient μ on optimal angle. "From the vehicle". Pumping frequency 18GHz.

In the "from the vehicle" case, the situation is even simpler. As it was shown in Section II B 3 the power conversion is optimal if we radiate both the pump and Stokes waves in the direction of the desired signal wave propagation. The estimated angular dependence (16) can be fitted with good accuracy to the numerical results using only one tuning coefficient C_{der}. It is shown that this coefficient weakly depends on the pumping frequency.

III. PRACTICAL USAGE OF THE OBTAINED RESULTS.

Let us now discuss the practical usage of this approach for receiving at and transmitting from the vehicle. For the "to the vehicle" case we consider the problem of receiving even

GPS signals. Let us estimate the resulting attenuation coefficient. Given a pump waveguide aperture of $3cm \times 3cm$ and a pump power of $3kW$, this gives $S_p = 3.3 \times 10^6 Wm^{-2}$. One can use the pulse regime. In this case, even for pulses $10^{-3}s$ long, every pulse still contains more than 10^6 periods of the low frequency signal and we can get much higher power flux $S_p^{pulse} = 3.3 \times 10^9 Wm^{-2}$. It gives us the attenuation coefficients $\mu_S S_p^{pulse}$

$$\mu_S S_p^{pulse} \simeq 0.73 \times 10^{-2}, \ \omega_p = 2\pi * 12GHz.$$
$$\mu_S S_p^{pulse} \simeq 2.1 \times 10^{-2}, \ \omega_p = 2\pi * 18GHz.$$

The usual level of a GPS signal at the Earth surface is about $-127.5dBm$ (1 Decibel per milliwatt is equal to $1dBm = 10\log_{10}(P/1mW)$). Indoors, one must use high sensitivity GPS receivers. Many general purpose chipsets have been available for several years. Presently, the market offers sensitivities $-157.5dBm$ (for example [5]). Using the definition of dBm one can see, that it is possible to receive a signal with an attenuation about 10^{-3}. Also it is possible to use a much bigger antenna on the vehicle than in the case of a handheld device. In this case, it is even possible to receive a signal using the continuous rather than pulsed regime for a klystron pump. So even at the angles far from optimal, one can receive GPS signals. Further, we used maximum value of the plasma thickness. If the plasma sheath is thinner, the angular dependence is broader.

Some characteristics of klystron amplifiers available on the open market are given here [5, 6].

Model	Frequency (GHz)	Power (kWatt)	Mass (kg)
LD4595	14.0-14.5	3	40
LD7126	17.3-18.4	2	27

In the "from the vehicle" case, because of sensitive land based receivers, all we need is to have a reasonable signal. Let us estimate an incoming power on some land based antenna. First of all, for any real antenna we have to take into account the decrease of a signal due to diffraction broadening. If the diameter of the land-based antenna (Figure 17) is D_0, the diameter of the signal flux after some long distance l will be

$$D(l) \simeq \frac{l\lambda}{2D_0}. \tag{25}$$

It means that if we have power flux at an antenna S_A, the power flux at the edge of the

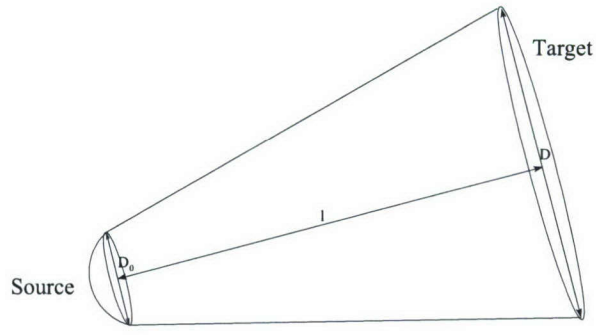

FIG. 17: Schematic plot of beam diffraction.

plasma after a distance l will be

$$S_0 \simeq S_A \left(\frac{2D_0^2}{l\lambda}\right)^2. \tag{26}$$

For example, for an antenna of the diameter equal to 5m, after 100km

$$S_0 \simeq 1.1 \times 10^{-5} S_A.$$

Now one can calculate the sensitivity of the receiver needed. Let us suppose that the signal beam outgoing from the vehicle has diameter $D_0 = 1m$, signal frequency $f = 2GHz$ and corresponding wave length $\lambda = 1.5 \times 10^{-1}m$, the land based antenna has a diameter $D_{LB} = 5m$ and is situated at a distance $l = 100km$. Using the previous results for diffraction, the pumping klystrons' powers from the table above and the expression $S_{out} = \mu S_p S_S$, one can get for the power on the land based receiver

$$S_{LB} \simeq S_{out} \left(\frac{2D_0^2}{l\lambda}\right)^2 = 1.8 \times 10^{-8} S_{out}. \tag{27}$$

We now list for two different frequencies, the corresponding powers in Watts at the receiving antenna.

$$\begin{aligned}
\omega_P &= 2\pi * 12GHz, \\
P_A &\simeq 1.8 \times 10^{-8} * 1.8 \times 10^{-16} * 9 \times 10^6 Wm^{-2} * 25m^2 \\
&\simeq 0.73 \times 10^{-15} W; \\
\omega_P &= 2\pi * 18GHz, \\
P_A &\simeq 1.8 \times 10^{-8} * 3.0 \times 10^{-17} * 4 \times 10^{12} Wm^{-2} * 25m^2 \\
&\simeq 0.54 \times 10^{-17} W.
\end{aligned}$$

The GPS receiver mentioned above has a sensitivity about $-160dBm \simeq 10^{-19}W$. Even with such a modest size of the antenna and ordinary klystrons one can receive the signal at almost any angle.

As a final remark one can conclude that proposed method for communication with and from the supersonic vehicle is realistic even using standard devices available on the open market.

IV. CONCLUSION.

We overcame the challenges described in the begining of this report. We achieved the complete success in estimation of applicability of the method we have proposed. Current technique can be utilized for communication with hypersonic vehicles even using current microwave devices available on the open market.

Following "Report of Department of Defense, Advisory Group on Electron Devices. Special Technology Area Review on Vacuum Electronics Technology for RF applications" at least since year 2000 much more powerfull and advanced klystrons are available for military purposes. It makes our estimations even more optimistic.

The code we created can be easyly used for simulations with an arbitary plasma density profile.

Results of the current work were published [7] in the Journal of Apllied Physics, which is a journal of such a respectable organization as American Institute of Physics.

APPENDIX A: RIGHT HAND SIDE OF THE GINZBURG EQUATION.

1. General case.

Consider the Ginzburg equation for a wave

$$H_3(y,z,t) = H_3(z)\mathrm{e}^{-\mathrm{i}\omega_3 t+\mathrm{i}k_3 y},$$

and calculate the right hand side of (2) in terms if the fields $H_1(y,z,t), H_2(y,z,t)$. In the "to the vehicle" case, H_1 will represent the pump wave, H_2 the signal wave and H_3 the Stokes wave. In the "from the vehicle" case, H_3 will be the signal and H_1 and H_2 the pump and signal carrying Stokes waves respectively. In all cases $\omega_3 = \omega_2 - \omega_1$, $k_3 = k_2 - k_1$. We find

$$\left[\nabla \times \vec{j}_{NL}(H_1, H_2, k_1, k_2, k_3, \omega_1, \omega_2, \omega_3)\right]_x =$$

$$= -\frac{e^3 n_0'(z) k_3}{2M^2\omega_3\left(1+\mathrm{i}\nu/\omega_3\right)}\left(\frac{1}{\varepsilon_1^*\left(1-\mathrm{i}\nu/\omega_1\right)\omega_1^2\varepsilon_2\left(1+\mathrm{i}\nu/\omega_2\right)\omega_2^2}\frac{\partial H_1^*}{\partial z}\frac{\partial H_2}{\partial z}+\right. \tag{A1}$$

$$\left.+\frac{k_1 k_2}{\varepsilon_1^*\left(1-\mathrm{i}\nu/\omega_1\right)\omega_1^2\varepsilon_2\left(1+\mathrm{i}\nu/\omega_2\right)\omega_2^2}H_1^* H_2\right)+$$

$$+\frac{e^3}{M^2}\left(\frac{k_2 k_1^2}{\left(1-\mathrm{i}\nu/\omega_1\right)\omega_1^3\varepsilon_2\left(1+\mathrm{i}\nu/\omega_2\right)\omega_2^2}\frac{\partial}{\partial z}\left(\frac{n_0(z)}{\varepsilon_1^*}\right)+\right.$$

$$\left.+\frac{k_2^2 k_1}{\left(1-\mathrm{i}\nu/\omega_1\right)\omega_2^3\varepsilon_1^*\left(1+\mathrm{i}\nu/\omega_2\right)\omega_1^2}\frac{\partial}{\partial z}\left(\frac{n_0(z)}{\varepsilon_2}\right)\right)H_1^* H_2 \tag{A2}$$

$$+\frac{e^3}{M^2}\left(\frac{1}{\omega_2^2\varepsilon_2\left(1+\mathrm{i}\nu/\omega_2\right)}\frac{\partial H_2}{\partial z}\frac{k_1}{\omega_1^3\left(1-\mathrm{i}\nu/\omega_1\right)}\frac{\partial}{\partial z}\left(H_1^*\frac{\partial}{\partial z}\left(\frac{n_0(z)}{\varepsilon_1^*}\right)\right)+\right.$$

$$\left.+\frac{1}{\omega_1^2\varepsilon_1^*\left(1-\mathrm{i}\nu/\omega_1\right)}\frac{\partial H_1^*}{\partial z}\frac{k_2}{\omega_2^3\left(1+\mathrm{i}\nu/\omega_2\right)}\frac{\partial}{\partial z}\left(H_2\frac{\partial}{\partial z}\left(\frac{n_0(z)}{\varepsilon_2}\right)\right)\right)- \tag{A3}$$

$$-\frac{\mu_0 e^3}{M^2}\left(\frac{k_2}{\omega_2^3\left(1+\mathrm{i}\nu/\omega_2\right)}\frac{\partial}{\partial z}\left(\frac{n_0(z)}{\varepsilon_2}\right)+\frac{k_1}{\omega_1^3\left(1-\mathrm{i}\nu/\omega_1\right)}\frac{\partial}{\partial z}\left(\frac{n_0(z)}{\varepsilon_1^*}\right)\right)H_1^* H_2. \tag{A4}$$

$$\left(\vec{j}_{NL}(H_1, H_2, k_1, k_2, k_3, \omega_1, \omega_2, \omega_3)\right)_y =$$

$$= \frac{e^3 n_0(z) k_3}{2M^2\omega_3\left(1+\mathrm{i}\nu/\omega_3\right)}\left(\frac{1}{\varepsilon_1^*\left(1-\mathrm{i}\nu/\omega_1\right)\omega_1^2\varepsilon_2\left(1+\mathrm{i}\nu/\omega_2\right)\omega_2^2}\frac{\partial H_1^*}{\partial z}\frac{\partial H_2}{\partial z}+\right. \tag{A5}$$

$$\left.+\frac{k_1 k_2}{\varepsilon_1^*\left(1-\mathrm{i}\nu/\omega_1\right)\omega_1^2\varepsilon_2\left(1+\mathrm{i}\nu/\omega_2\right)\omega_2^2}H_1^* H_2\right)-$$

$$-\frac{e^3}{M^2}\left(\frac{1}{\omega_2^2\varepsilon_2\left(1+\mathrm{i}\nu/\omega_2\right)}\frac{\partial H_2}{\partial z}\frac{k_1}{\omega_1^3\left(1-\mathrm{i}\nu/\omega_1\right)}H_1^*\frac{\partial}{\partial z}\left(\frac{n_0(z)}{\varepsilon_1^*}\right)+\right.$$

$$\left.+\frac{1}{\omega_1^2\varepsilon_1^*\left(1-\mathrm{i}\nu/\omega_1\right)}\frac{\partial H_1^*}{\partial z}\frac{k_2}{\omega_2^3\left(1+\mathrm{i}\nu/\omega_2\right)}H_2\frac{\partial}{\partial z}\left(\frac{n_0(z)}{\varepsilon_2}\right)\right). \tag{A6}$$

2. Approximate right hand side. "To the vehicle" case.

In the "to the vehicle" case, the main contribution comes from the terms containing poles

$$\left[\nabla \times \vec{j}_{NL}(H, H_p, k, k_p, k_S, \omega, \omega_p, \omega_S)\right]_x \simeq \tag{A7}$$

$$\simeq \frac{e^3}{M^2}\frac{k_p k^2}{\left(1-\mathrm{i}\nu/\omega_p\right)\omega^3\varepsilon_p\left(1+\mathrm{i}\nu/\omega_p\right)\omega_p^2}\frac{\partial}{\partial z}\left(\frac{n_0(z)}{\varepsilon^*}\right)H^* H_p+$$

$$+\frac{e^3}{M^2}\frac{1}{\omega_p^2\varepsilon_p\left(1+\mathrm{i}\nu/\omega_p\right)}\frac{\partial H_p}{\partial z}\frac{k}{\omega^3\left(1-\mathrm{i}\nu/\omega\right)}\frac{\partial}{\partial z}\left(H^*\frac{\partial}{\partial z}\left(\frac{n_0(z)}{\varepsilon^*}\right)\right)-$$

$$-\frac{\mu_0 e^3}{M^2}\frac{k}{\omega^3\left(1-\mathrm{i}\nu/\omega\right)}\frac{\partial}{\partial z}\left(\frac{n_0(z)}{\varepsilon^*}\right)H^* H_p. \tag{A8}$$

Assume that the high frequency pumping wave remains undisturbed. Then

$$H_p(y,z,t) = H_p \mathrm{e}^{\mathrm{i}(k_p y - \kappa_p z - \omega t)},$$

we find

$$f_S(z) = -\left[\nabla \times \vec{j}_{NL}\right]_x \mathrm{e}^{-\mathrm{i}\kappa_p z}$$

and

$$C_1(R) = \frac{1}{2\mathrm{i}\kappa_S} \int_{-L}^{R} f_S(y) \mathrm{e}^{-\mathrm{i}\kappa_S y} dy \simeq$$
$$\frac{1}{2\mathrm{i}\kappa_S} \int_{-\infty}^{+\infty} f_S(y) \mathrm{e}^{-\mathrm{i}\kappa_S y} dy.$$

After several integrations by parts in the second term of $\left[\nabla \times \vec{j}_{NL}\right]_x$, taking into account $k_S = k_p - k$, one finds

$$C_1(R) \simeq \frac{-ik}{2\kappa_S} \frac{e^3 H_p H^*}{M^2 \varepsilon_0 \omega_p^2 \omega^3} \left(k_p(k_p - k_S) + (\kappa_p + \right. \tag{A9}$$
$$\left. \kappa_S)\kappa_p - \frac{\omega_p^2}{c^2}\right) \int_{-\infty}^{+\infty} \frac{\partial}{\partial z}\left(\frac{n_0(z)}{\varepsilon^*}\right) \mathrm{e}^{-\mathrm{i}(\kappa_S + \kappa_p)z} \mathrm{d}z.$$

For most pumping angles, and using the fact that $\omega_p \gg \omega$, one can substitute $\omega_S \simeq \omega_p$ and consider incidence angles of pumping and Stokes wave to be close in absolute value. Following Fig. 1 the pumping incidence angle is θ and low frequency signal incidence angle is ϕ.

$$C_1(R) \simeq \frac{-ik}{2\kappa_S} \frac{e^3 H_p}{M^2 \varepsilon_0 \omega_p^2 \omega^3} \frac{\omega_p^2}{c^2} \cos(2\theta) \tag{A10}$$
$$\int_{-\infty}^{+\infty} \frac{\partial}{\partial z}\left(\frac{n_0(z)}{\varepsilon^*}\right) H^* \mathrm{e}^{-\mathrm{i}(\kappa_S + \kappa_p)z} \mathrm{d}z.$$

Using integration by parts once more one can get

$$C_1(R) \simeq \frac{(\kappa_p + \kappa_S)}{2\kappa_S} \frac{e^3 H_p}{M^2 \varepsilon_0 c^3 \omega^2} \cos(2\theta) \sin(\phi) \times \tag{A11}$$
$$\times \int_{-\infty}^{+\infty} \left(\frac{n_0(z)}{\varepsilon^*}\right) H^* \mathrm{e}^{-\mathrm{i}(\kappa_S + \kappa_p)z} \mathrm{d}z.$$

Calculating this integral by residues and taking into account

$$n_0(z) \simeq n_0(z=0) = n_0 \frac{L}{L+R} = n_0 \frac{\omega^2}{\omega_L^2},$$
$$\frac{\varepsilon_0}{\varepsilon} = -\frac{L}{z + i\delta},\ \delta = \mathrm{i}\frac{\nu}{\omega} L,$$

we finally get

$$C_1(R) \simeq 2\pi \mathrm{i} \frac{e^3 n_0 L}{M^2 \varepsilon_0^2 c^3 \omega_L^2} \cos(2\theta) \sin(\phi) H_p H^*(0) =$$
$$= 2\pi \mathrm{i} \frac{eL}{Mc^2} \frac{1}{\varepsilon_0 c} \cos(2\theta) \sin(\phi) H_p H^*(0).$$

[1] S. Nazarenko, A. C. Newell, V. E. Zakharov, Phys. Plasmas, **1**, 9, 2834 (1994).

[2] S. Nazarenko, A. C. Newell, A. M. Rubenchik, AGU Radio Science, **3**, 1 (1994).

[3] S. Nazarenko, A. C. Newell, A. M. Rubenchik, Phys. Lett. A, **197**, 159 (1995).

[4] V. L. Ginzbug, "The propagation of electromagnetic waves in plasmas", 2nd rev. and enl. ed., International Series of Monographs in Electromagnetic Waves, Oxford: Pergamon (1970)

[5] Fujitsu Microelectronics Asia Pte Ltd.
http://www.fujitsu.com/ph/news/pr/fmal_20040722.html

[6] NEC Microwave Tube, Ltd.
http://www.nec-mwt.com/english/klyamp_es.html

[7] A. O. Korotkevich, A. C. Newell, V. E. Zakharov, J. Appl. Phys., **102**, 8, 083305 (2007).